Studies on Manganese(II) Complexes of *N*-Benzimidazole-Functionalized 1,4,7-Triazacyclononane: Crystal Structures, Properties and Combined Superoxide Dismutase and Catalase Functions

Qing-Xiang Li,[a,b] Qin-Hui Luo,*[a] Yi-Zhi Li,*[a] Zhi-Quan Pan,[a,b] and Meng-Chang Shen[a]

Keywords: Enzyme models / Manganese / N ligands / Superoxide dismutase

Two new manganese(II) complexes $[MnL^1Cl_2]$ and $[MnL^2Cl]ClO_4$·MeOH were synthesized [L^1 = 1-(benzimidazol-2-ylmethyl)-1,4,7-triazacyclononane; L^2 = 1,4-bis(benzimidazol-2-ylmethyl)-1,4,7-triazacyclonone) and characterized by standard physical methods. The new complexes have better stability than the parent complex due to the introduction of benzimidazole groups on the backbone of tacn. The complexes were studied as superoxide dismutase (SOD) mimics by the riboflavin photoreduction method at pH 7.4. In basic or weakly basic solutions, the complexes decompose hydrogen peroxide catalytically, and possess the combined functions of SOD and catalase.

Introduction

Superoxide dismutase (SOD) efficiently catalyzes the dismutation of superoxide anion ($O_2^{\cdot-}$) to oxygen and hydrogen peroxide,[1,2] which is subsequently disproportionated into water and oxygen by catalase[3] (CAT).

$$O_2^{\cdot-} + 2\,H^+ + e^- \rightarrow H_2O_2$$
$$2\,H_2O_2 \rightarrow 2\,H_2O + O_2$$

Both SOD and CAT play important roles in the protection of cells against the toxicity of oxygen.[3] Manganese is involved in many biological processes,[4] such as hydrogenperoxide decomposition and superoxide dismutation etc., and is found at the active centers of MnSOD[5,6] and MnCAT.[5]

In MnSOD the manganese has a trigonal-bipyramidal coordination environment with three histidine groups and one monodentate carboxylate group,[6] whereas MnCAT may effectively catalyze the disproportionation of H_2O_2 by using a μ-oxo/hydroxo-bis(μ-carboxylate)dimanganese structural unit as the active site.[5,7,8] Recently, various dinuclear manganese-based catalase mimics[9] that decompose hydrogen peroxide have been screened as catalysts for low-temperature bleaching[10] and for organic syntheses.[11] The manganese complexes used as mimics of MnSOD are more suitable than Cu_2Zn_2SOD because manganese has a lower toxicity in mammalian systems.[12] Recently, various mononuclear manganese complexes have been selected for pharmaceutical uses,[13] such as manganese complexes with Schiff-base ligands,[14] porphyrins, 1,4,7,10,13-pentazacylic pentadecane derivatives,[15,16] and so on.[17] Among these, a class of complexes with combined SOD and catalase functions have attracted many people's attention: complexes such as [Mn(salen)Cl] and [Mn(vanl)Cl] (salen and vanl are the [1+2] condensates of ethylenediamine with salicyladehyde or vanillin, respectively) exhibit both SOD and catalase activities, catalytically destroying both superoxide anion and hydrogen peroxide. Due to their novel combined functions, they have been suggested to serve as therapeutic agents.[18–20]

An attractive property of the tridentate macrocycle 1,4,7-triazacyclonone (tacn) is its ability to form thermodynamically stable redox-active manganese complexes.[21,22] In this paper, this ligand has been further modified. Two new manganese(II) complexes $[MnL^1Cl_2]$ **1** and $[MnL^2Cl]ClO_4$·MeOH **2** [L^1 = 1-(benzimidazol-2-yl-methyl)-1,4,7-tacn, L^2 = 1,4-bis(benzimidazol-2-yl-methyl)-1,4,7-tacn] have been synthesized and characterized by stndard physical methods. Interestingly, the two complexes exhibit SOD activities, catalytically dismutating $O_2^{\cdot-}$, and possess the combined functions of SOD and catase.

Results and Discussion

Characterization

Both complexes possess similar spectroscopic features. In the IR spectra the strong bands at 3415 and 3384 cm^{-1} are

[a] Coordination Chemistry Institute, State Key Laboratory of Coordination Chemistry,
Nanjing 210093, P. R. China
E-mail: qhluo@jlonline.com
[b] School of Chemical engineering & Pharmacy, Wuhan Institute of Chemical Technology
430073, P. R. China

due to the N−H stretching vibration of complexes **1** and **2**, respectively. The medium-strong bands at about 750 cm^{-1} are designated as skeleton stretching of the aromatic ring. Complex **2** exhibits a strong band at 1107 cm^{-1}, showing the presence of ClO_4^-.

In the electronic spectra, the absorptions of the two complexes in the range of 279−272 nm and at 244 nm are characteristic of the B band and E_2(K) band of *o*-phenylene, respectively. The values of the molar conductivities indicate that both complexes are 1:1 electrolytes in MeCN solution.

The magnetic susceptibilities of the two complexes show that the manganese in each complex has a high-spin, d^5 configuration.

The EPR spectra of complex **2** in MeOH solution at room temperature and 110 K are shown in Figure 1. Figure 1 (see a) exhibits a six-line spectrum, typical of mononuclear Mn^{II}, centered at 3496 G, with $g = 1.999$ and a hyperfine coupling constant, A, of 88×10^{-4} cm^{-1} associated with the $I = 5/2$ nuclear spin of ^{55}Mn. This signal results from allowed transitions ($\Delta m_s = \pm 1$, $\Delta m_I = 0$). In the spectrum at 110 K (see b in Figure 1) it is possible to see the weak, forbidden transition signals between the six intense signals.

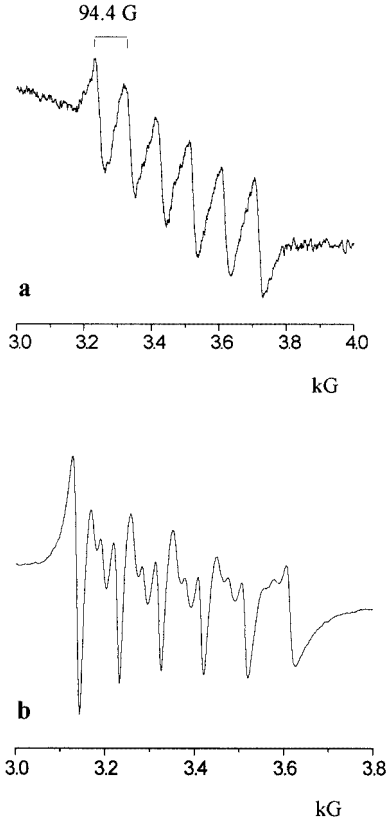

Figure 1. EPR spectra of the complex $[MnL^2Cl]ClO_4 \cdot MeOH$ in methanol (1.0×10^{-2} mol·dm^{-3}): (a) at room temperature; (b) at 110 K; microwave frequency: 948 GHz; microwave power: 20 mW; gain: 1.0×10^5; scan range: 2000 G; time constant: 100 s; scan time: 100 s

The positive-ion electrospray (ES) mass spectra of $[MnL^1Cl_2]$ **1** and $[MnL^2Cl]ClO_4 \cdot MeOH$ **2** in MeOH solution were also recorded. The results are listed in Table 1. These peaks are due to loss of one or two chloride anions, formation of dinuclear Mn^{II} species with two chloride anions as bridging ligands, or binding of solvent molecules. The loss of chloride anions shows the weak interaction between the Cl^- ion and manganese(II), which would favor the attack of species with low molecular weight, such as superoxide anion. No peaks of ligands or their fragments were found in the mass spectra of the two complexes, and their simplicity is attributed to the thermodynamic stability and kinetic inertness of the two complexes.[22] No peaks were found due to the loss of Mn^{2+} ion or the pendant arm. This indicates that both complexes are stable under the experimental conditions.

Electrochemical Properties

The redox behavior of **1** and **2** was studied by cyclic voltammetry in aqueous solution and in MeOH solution for **1** and **2**, respectively. During scanning from −0.3 V to +0.8 V the CV diagram of **1** in aqueous solution displays one pair of anodic and cathodic peaks with peak potentials of $E_{pa} = 0.411$ V and $E_{pc} = -0.109$ V (vs. SCE) respectively. The value of the half-wave potential, $E_{1/2}$, was calculated to be 0.151 V. The anodic peak current (i_p) is almost equal to the cathodic one. In the same range of potential scan rate (v), the $i_p/v^{1/2}$ ratio is kept constant. The peak separation between the anodic and cathodic peaks at a scan rate 50 mV·s^{-1} is 520 mV. These features are indicative of a quasi-reversible M^{II}/Mn^{III} redox process. Other redox peaks were not found at a more negative potential, implying that the macrocycle effect stabilizes the Mn^{III} oxidation state. Complex **2** shows two pairs of quasi-reversible anodic and cathodic peaks with $E^1_{1/2} = 0.527$ V for first pair of peaks and $E^2_{1/2} = 0.697$ V for the second pair of peaks (Figure 2); they are assigned to the Mn^{III}/Mn^{II} and Mn^{IV}/Mn^{III} couples, respectively.

According to the redox potential of $\cdot O_2^-$ in neutral solution

$O_2 + e^- \rightarrow \cdot O_2^-$; $E^o_{pH7} = -0.16$ V (vs. NHE)
$\cdot O_2^- + 2\,H^+ + e^- \rightarrow H_2O_2$; $E^o_{pH7} = +0.89$ V (vs. NHE)

in order to act as a catalyst of $\cdot O_2^-$ disproportionation, the complexes must have a half-wave potential falling between two values. The half-wave potentials for complex **1** [$E_{1/2} = 0.392$ V (vs. NHE)] and complex **2** [$E^1_{1/2} = 0.769$ V (vs. NHE)] both fall between −0.16 V and +0.89 V (see Equation 3 and 4[23]), therefore both complexes can be oxidized by $\cdot O_2^-$ and their oxidized form can be re-reduced by $\cdot O_2^-$ to finish the catalytic cycles, as follows:

$Mn^{II} + \cdot O_2^- + 2H^+ \rightarrow Mn^{III} + H_2O_2$
$Mn^{III} + \cdot O_2^- \rightarrow Mn^{II} + O_2$

For the second pair of peaks of complex **2**, the half-wave potential is higher than +0.89 V [$E^2_{1/2} = 0.939$ V (NHE)], indicating that $\cdot O_2^-$ cannot oxidize Mn^{III} to Mn^{IV} in this

Table 1. Peak assignments of complexes **1** and **2**

$[MnL^1Cl_2]$ (**1**)		$[MnL^2Cl]ClO_4$·MeOH (**2**)	
349.2 (100)[a]	$[MnL^1Cl]^+$	479.2 (100)	$[MnL^2Cl]^+$
172.9 (22)	$[MnL^1 + MeOH]^{2+}$	222.2 (24)	$[MnL^2]^{2+}$
732.9 (13)	$[Mn_2L^1{}_2Cl_2 + 0.5MeOH + OH^-]^+$	609.2 (13)	$[MnL^2 + 4MeOH]^+$
		237.7 (9)	$[MnL^2 + MeOH]^{2+}$

[a] The relative abundance is given in parentheses.

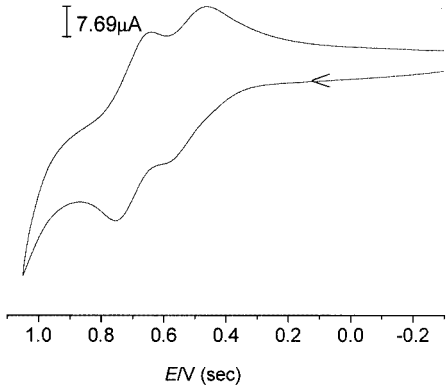

Figure 2. Cyclic voltammogram of complex **2** in MeOH solution; concentration: 1.0×10^{-3} mol·dm^3 (scan rate 100 mV·s^{-1})

complex. Therefore the catalytic cycle occurs only between Mn^{II} and Mn^{III}; this is similar to MnSOD.

pH Titration

The coordinating ability of the ligands towards Mn^{2+} was studied by means of pH titration of a solution containing L^1·3HCl (or L^2·3HCl) and $Mn(NO_3)_2$ in equimolar amounts. To avoid precipitation of manganese(II) complexes of L^2 in aqueous solution during titration by NaOH, the experiments were carried out in dioxane/water (7:3, v/v). The titration curves of ligand L^1·3HCl (1) and L^1·3HCl plus Mn^{2+} ion (2) in aqueous solution are shown in Figure 3. The first inflexions of the two curves are at about $a = 1$ (a denotes the number of mols of NaOH added per mol of ligand), showing that one mol of the acid was titrated by base. For curve (2) in Figure 3 a very long buffer region at about $a = 1-3$, indicates the formation of the dominant species $[Mn(L^1)]^{2+}$, after which a slow inflexion occurs corresponding to the coexistence of $[MnL^1(OH)]^+$ and $[MnL^1(OH)_2]$ species, implying that the hydroxyl ions are bound to the unoccupied coordination sites. Assuming the coexistence of $[Mn(L^1)]^{2+}$, $[MnL^1(OH)]^+$ and $[MnL^1(OH)_2]$, the equilibrium constants (Table 2) were obtained by a curve fitting procedure. Comparing the equilibrium constants of complexes **1** and **2** with those of their parent complexes, which have no benzimidazole groups on the tacn backbone, we can see that the species $[MnL]^{2+}$ for 1 and 2 have better stability than the parent complex. The species-distribution curves of curve (2) are shown in Figure 4. The distribution curves of complexes **1** and **2** show that, at physiological pH (7.4), an $[MnL^1(OH)]^+$ species still predominates for both L^1 and L^2, implying that the vacant site at Mn^{II} atom is suitable for the coordination of hydroxyl ion. The percentage of free Mn^{2+} is less than 0.07% and 0.08% for L^1 and L^2, respectively. This means that the ligands have a relatively strong coordinating ability to manganese(II).

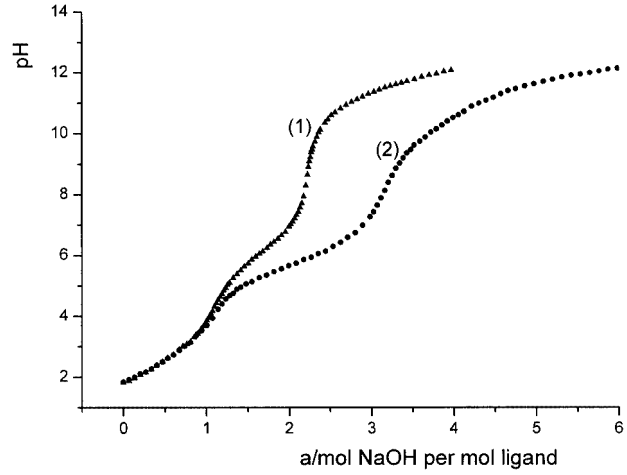

Figure 3. pH Titration curves in aqueous solutions: (1) $[L^1·3HCl] = 0.002496$ mol·dm^{-3}; (2) $[L^1·3HCl] = [Mn^{2+}] = 0.002504$ mol·dm^{-3}; $I = 0.1$ mol·dm^{-3} (KNO_3), 25 °C

Crystal Structures of the Complexes

[MnL¹Cl₂]

The crystal data of complexes **1** and **2** are listed in the Exp. Sect. The structure of the $[MnL^1Cl_2]$ is shown in Figure 5 (a), and selected bond lengths and angles are given in Table 3. In complex **1**, each Mn^{II} atom is coordinated by four nitrogen atoms of the triazacycle [N(1), N(2), N(3)], with average bond lengths of 2.292 Å, one benzimidazole nitrogen atom N(4), and two chloride ions. The Mn−N(4) bond length is 2.214 Å, and is the shortest of the Mn−N bonds. This indicates that the nitrogen atom of the benzimidazole group has a stronger coordination ability to Mn^{II} than the nitrogens of the triazacycle and plays an important role in increasing the stability of the complex. The two Mn−Cl bond lengths [2.5298(11) Å for Cl (1) and 2.4067 Å for Cl (2)] are longer than the Mn−N bond lengths, therefore these Cl^- anions are able to be detached from the Mn^{II} atom in solution, as proved by the ES-MS experiment.

Table 2. Equilibrium constants at 25 °C; I = 0.20 mol·dm^{-3} (KNO_3)

Reaction	L^1	L^2 [a]	[9]aneN$_3$ [21c]
$L + H^+ \rightleftarrows [HL]^+$	11.01± 0.02	9.16 ± 0.01	10.42
$[HL]^+ + H^+ \rightleftarrows [H_2L]^{2+}$	5.74 ± 0.01	3.39 ± 0.02	6.82
$[H_2L]^{2+} + H^+ \rightleftarrows [H_3L]^{3+}$	3.50 ± 0.02	1.02 ± 0.01	very small
$Mn^{2+} + L \rightleftarrows [MnL]^{2+}$	9.95 ± 0.01	6.52 ± 0.01	5.8
$Mn^{2+} + L + OH^- \rightleftarrows [MnL(OH)]^+$	3.50 ± 0.02	2.69 ± 0.02	3.6
$Mn^{2+} + L + 2OH^- \rightleftarrows [MnL(OH)_2]$	−5.52 ± 0.03	−6.73 ± 0.02	

[a] Experiments for L^2 were carried out in dioxane/water solution (7:3, v/v).

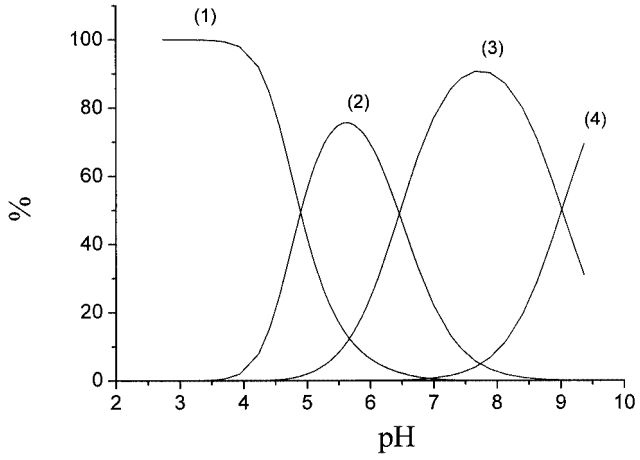

Figure 4. Species distribution curves for curve (2) of Figure 3: (1) Mn^{2+}; (2) $[Mn(L^1)]^{2+}$; (3) $[MnL^1(OH)]^+$; (4) $[MnL^1(OH)_2]$

The Mn^{II} is located at the center of a distorted octahedron, with the Cl(1) and N(2) atoms located in the axial direction and Cl(2), N(1), N(3) and N(4) located in the equatorial plane. The Cl(1)−Mn−N(2) angle is 164.45(7)°. The least-squares plane is composed of Cl(2), N(1), N(3), and N(4), with the Mn^{II} atom lying 0.6973 Å out of this plane. The dihedral angle between the benzimidazole plane and the equatorial plane is 11.5°.

Table 3. Selected bond lengths (Å) and angles (°) of complex **1**

Mn(1)−Cl(1)	2.5298(11)	Mn(1)−N(1)	2.389(2)
Mn(1)−N(2)	2.304(2)	Mn(1)−N(3)	2.261(3)
Mn(1)−N(4)	2.214(3)	Mn(1)−Cl(2)	2.4067(11)
Cl(1)−Mn(1)−N(1)	91.25(6)	Cl(1)−Mn(1)−N(2)	164.45(7)
Cl(1)−Mn(1)−N(3)	94.57(9)	Cl(1)−Mn(1)−N(4)	89.70(7)
Cl(1)−Mn(1)−Cl(2)	99.95(4)	Cl(2)−Mn(1)−N(1)	167.53(7)
Cl(2)−Mn(1)−N(2)	93.73(7)	Cl(2)−Mn(1)−N(3)	98.18(7)
Cl(2)−Mn(1)−N(4)	111.34(8)	N(1)−Mn(1)−N(2)	74.49(9)
N(1)−Mn(1)−N(3)	75.30(9)	N(1)−Mn(1)−N(4)	73.88(10)
N(2)−Mn(1)−N(3)	76.07(10)	N(2)−Mn(1)−N(4)	92.18(10)
N(3)−Mn(1)−N(4)	148.96(10)		

[MnL^{2}Cl]ClO$_4$·MeOH

The structure of the complex cation $[MnL^2Cl]^+$ is shown in Figure 5 (b); selected bond lengths and angles are given in Table 4. The coordination environment of **2** is very similar to that of **1**, except that one chloride anion has been replaced by a nitrogen atom of another benzimidazol-2-yl-

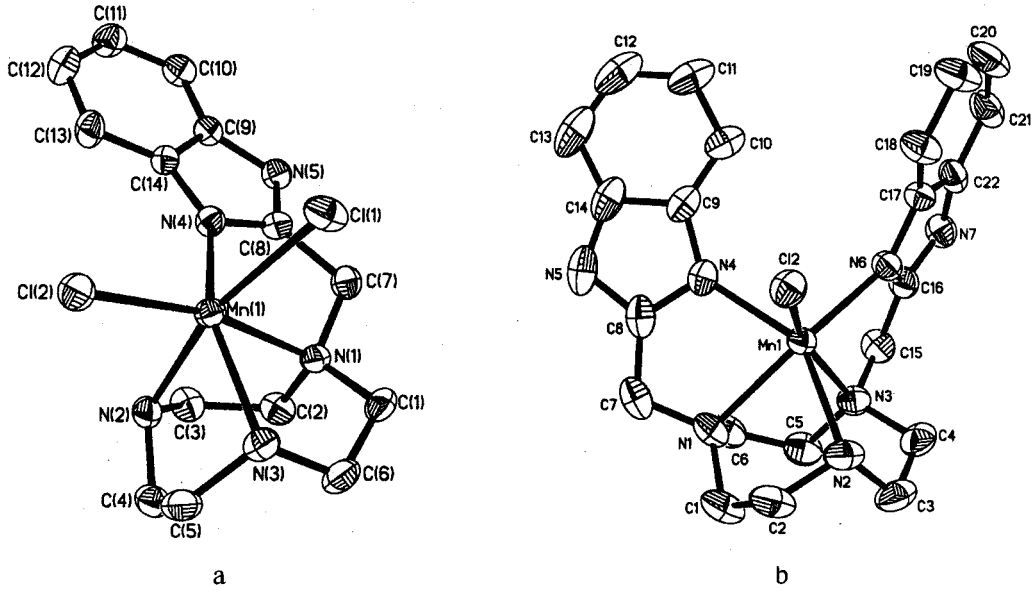

Figure 5. Crystal structure of $[MnL^1Cl_2]$ (a) and the $[MnL^2Cl]^+$ cation (b)

Table 4. Selected bond lengths (Å) and angles (°) of complex **2**

Mn(1)−Cl(2)	2.4668(7)	Mn(1)−N(1)	2.407(2)
Mn(1)−N(2)	2.228(2)	Mn(1)−N(3)	2.376(2)
Mn(1)−N(4)	2.202(2)	Mn(1)−N(6)	2.1723(19)
Cl(2)−Mn(1)−N(1)	116.20(7)	Cl(2)−Mn(1)−N(2)	88.04(7)
Cl(2)−Mn(1)−N(3)	158.13(6)	Cl(2)−Mn(1)−N(4)	92.82(6)
Cl(2)−Mn(1)−N(6)	101.17(6)	N(1)−Mn(1)−N(2)	75.00(8)
N(1)−Mn(1)−N(3)	74.15(8)	N(1)−Mn(1)−N(4)	72.38(8)
N(1)−Mn(1)−N(6)	141.65(8)	N(2)−Mn(1)−N(3)	75.80(8)
N(2)−Mn(1)−N(4)	143.96(8)	N(2)−Mn(1)−N(6)	116.55(8)
N(3)−Mn(1)−N(4)	108.94(8)	N(3)−Mn(1)−N(6)	74.00(7)
N(4)−Mn(1)−N(6)	98.64(8)		

methyl ligand. The Mn−Cl bond length is 2.4668(7) Å. The Mn^{II} atom is also located at the center of a distorted octa5-hedron as in **1**. The atoms N(1), N(2) and N(3) of the aza-macrocycle constitute a face of the octahedron, and two nitrogen atoms [N(4), N(6)] of the two benzimidazol-2-yl-methyls and the Cl^- anion compose the opposite face. Cl(2) and N(3) are located in the axial direction with a Cl(2)−Mn−N(3) angle of 158.13(6)°. The equatorial plane is composed of N(1), N(2), N(4) and N(6), and the Mn^{II} atom is 0.3893 Å out of this plane. The dihedral angle between the equatorial plane and one of the benzimidazole planes [N(4), N(5), C(8)−C(14)] is 164.2°, and that between the equatorial plane and the other benzimidazole plane [N(6), N(7), C(16)−C(22)] is 89.3°. The dihedral angle between the two benzimidazole planes is 76.1°. The two benzimidazole groups encapsulate Mn^{II} to form a hydrophobic packet with a channel.

SOD Activities of the Complexes

The SOD activities of the complexes were studied in aqueous solutions of phosphate buffer (pH 7.4) by the riboflavin photoreduction method.[24] Both complexes inhibit the reduction of nitroblue tetrazolium chloride, depending on their concentrations. The activity was obtained by plotting the percentage of inhibiting NBT reduction, *f* (%), against the concentration of the complex, *C*. The plot for complex **2** is shown in Figure 6. The activities of complexes **1** and **2**, together with those for $Mn(ClO_4)_2$ and Cu_2Zn_2SOD determined under the same conditions, are listed in Table 5. The activities of **1** and **2** are of the same order of magnitude as that of Mn^{2+} ion, but these high activities are not due to free Mn^{2+} ion produced by dissociation of the complexes. The free Mn^{2+} ion can be ignored in solution, as proved by the pH titration. The activities of the complexes are about 1% of that of Cu_2Zn_2SOD.

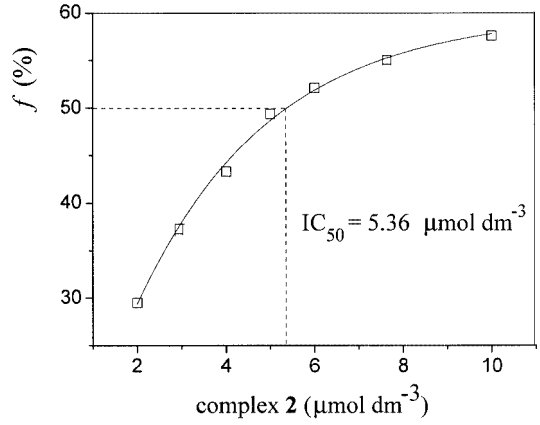

Figure 6. A plot of inhibition percentage (*f*%) vs. concentration for complex **2**

The complexes were also studied by the addition of various concentrations of bovine serum albumin (BSA) to the tested solutions in order to further prove the stability of the complexes under protein conditions. It was found that the concentration of BSA has no effect on the activities of the two complexes until it reached a value of 0.2 mg/mL. The ES mass spectra and X-ray structural analyses of the two complexes show that the binding of chloride anions to the Mn^{II} center is rather weak, and therefore it is likely that the Cl^- could become partially detached in solution. As the concentration of $^{\cdot}O_2^-$ in the solution much higher than that of OH^- at pH 7.4, the vacant coordination sites are open to attack by $^{\cdot}O_2^-$. The benzimidazole groups are similar to the hydrophobic residues of MnSOD. In complex **2**, with two benzimidazole groups, the benzimidazole groups surround the metal ion to form a hydrophobic channel which favors the attack of $^{\cdot}O_2^-$; complex **2** therefore displays higher SOD activity.

Reactivity with Hydrogen Peroxide

The catalytic activity of complexes **1** and **2** towards hydrogen peroxide was investigated in methanol/water solutions (1:5, v/v) and in aqueous solutions, respectively. The evolution of dioxygen was followed manometrically as a function of time at room temperature. The O_2-evolution curve for complex **1** is shown in Figure 7. In the absence of NaOH, the complex decomposes hydrogen peroxide very slowly (Figure 7, curve 1) corresponding to the self-decomposition of H_2O_2. After 15 min only 7.0% of the total H_2O_2 had been decomposed. Previous authors have re-

Table 5. The activities of complexes **1** and **2**

Compounds	**1**	**2**	$Mn(ClO_4)_2{\cdot}6H_2O$	Cu_2Zn_2SOD
IC_{50} (μmol·dm^{-3})	8.33 (8.41)[a]	5.36 (5.88)[a]	3.56	0.06
Relative activity (%)	0.7	1.1	1.7	100

[a] The numbers in parentheses are the activities assayed upon addition of a further 0.2 mg/L of BSA.

Table 6. The kinetic data of H_2O_2 decomposition by the complexes at 25 °C

Complex	Solvent	$C_{complex}$ ($\times 10^4$ mol·dm^{-3})	$C_{H^2O^2}$ (mol·dm^{-3})	C_{NaOH} ($\times 10^3$ mol·dm^{-3})	υ_0 ($\times 10^4$ mol·min^{-1})	υ' (s^{-1})	Turnover (t = 15 min)	H_2O_2 (%) (t = 15 min)
1	MeOH/H_2O	8.45	0.535	4.84	4.24	5.58	606	95.7%
2	MeOH/H_2O	8.50	0.535	5.69	1.55	2.03	609	96.8%
1	H_2O	9.89	0.487	5.43	6.63	6.70	483	98.2%

ported that the addition of an organic base accelerates significantly the catalytic decomposition of hydrogen peroxide by manganese complexes.[25] However, in this experiment organic bases such as pyridine, imidazole and acetate anion did not increase the rate of O_2 evolution. Interestingly, the rate of O_2 evolution increased with an increase of the concentration of NaOH, and at a molar ratio of NaOH to complex **1** of 1.68 (pH 7.38), the percentage of decomposed H_2O_2 reached 90% after 15 min. When the molar ratio of NaOH to complex **1** was equal to 5.73 (pH 11.03), we obtained an initial turnover rate, υ' of 5.58 mol H_2O_2/mol catalyst·s^{-1} and a turnover number (number of mols of H_2O_2 decomposed per mol catalyst) of 606 (after the reaction stopped). The kinetic data for H_2O_2 decomposition by the complexes are listed in Table 6, where it can be seen that the value of υ' of complex **1** is higher than that of complex **2** in MeOH/water solvent, although its turnover is lower, because the formation of a dinuclear manganese complex as the active species (see below) is difficult for complex **2** due to the steric hindrance of the two benzimidazole groups, however, the turnover of complex **2** is higher because the active species of **2** does not easily decompose. In aqueous solution, complex **1** has a higher value of υ' and a lower turnover number than in mixed solvent, probably because both H_2O_2 and the active species of complex **1** have a low stability in aqueous solution, resulting in a high catalytic activity and a low turnover. The υ' values of complex **1** in aqueous solution and mixed solvent are close to that of the dinuclear manganese complex with the *N*,*N*′,*N*′′-trimethyl-1,4,7-triazacyclononane ligand[26] (υ' = 5.55 s^{-1}), although the turnover is lower. To date, the dinuclear manganese complexes reported[4] have rate values that range from 0.013[28] to 50 s^{-1}.[27] The values of υ' for complexes **1** and **2** therefore fall at the high end of the range of those reported previously.

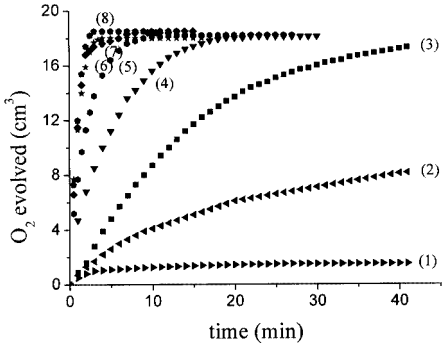

Figure 7. Curves of oxygen evolution for the catalytic disproportionation of H_2O_2 by $[MnL^1Cl_2]$ (**1**) in methanol/water solution (1:5, v/v); $C_{complex}$: 8.45 × 10^{-4} mol·dm^{-3}; C_{NaOH}: (1) 0 (pH 4.71); (2) 5.12 × 10^{-4} (pH 5.06); (3) 7.11 × 10^{-4} (pH 6.02); (4) 1.42 × 10^{-3} (pH 7.38); (5) 1.99 × 10^{-3} (pH 8.31); (6) 3.42 × 10^{-3} (pH 9.44); (7) 4.27 × 10^{-3} (pH 10.57); (8) 4.84 × 10^{-3} (pH 11.03)

Active Intermediates

A number of the dinuclear manganese complexes with oxygen or hydroxyl bridges reported previously exhibit significant rate enhancement for the disproportionation of hydrogen peroxide in the presence of an exogenous base. It has been proposed that this effect is due to the base-facilitated deprotonation of H_2O_2 in the course of the coordination of hydrogen peroxide to the manganese center. In our experiment, however, this is not the case as the concentration of H_2O_2 is very much higher (several hundred times) than those of complex and NaOH. Therefore, the main function of the added NaOH is not capturing a proton from H_2O_2.

The active intermediates in the catalytic decomposition reactions of hydrogen peroxide by the manganese complexes could not be isolated from the solutions. Therefore, in order to trap the active species, the ES mass spectrum of complex **1** plus H_2O_2 and NaOH in MeOH solution was recorded (Figure 8). The peak assignments are shown in Table 7, in which all species derived from complex **1** are oxygen-bridged or hydroxyl-bridged binuclear complex cations and the oxidation state of manganese is +2 or +3. According to these results, a possible mechanism of hydrogen peroxide dismutation is suggested in Scheme 1.

In step 1 the Cl^- ligand in complex 1 is substituted by water molecules, and in step 2 complexes containing one or two hydroxyl-bridged units are formed in basic solution. In step 3 the water molecules are replaced by H_2O_2, followed by an intramolecular electron transfer (step 4). Finally, the intermediate reacts further with H_2O_2 and the catalytic cycle is completed (step 5).

For complex **2**, the ES mass spectrum obtained under the same conditions as **1** is different (Table 8) as only a few molecules of complex **2** are changed into hydroxyl-bridged or oxygen-bridged binuclear manganese units due to the steric hindrance of the two benzimidazole groups; the manganese therefore exists in the Mn^{II}, Mn^{III} and Mn^{IV} oxidation states. The variation of oxidation state for complexes **1** and **2** during the disproportionation of hydrogen peroxide is in agreement with the results obtained by cyclic voltammetry.

It is remarkable that irrespective of whether they are dissolved in MeOH/water or only in water at about pH 7.3,

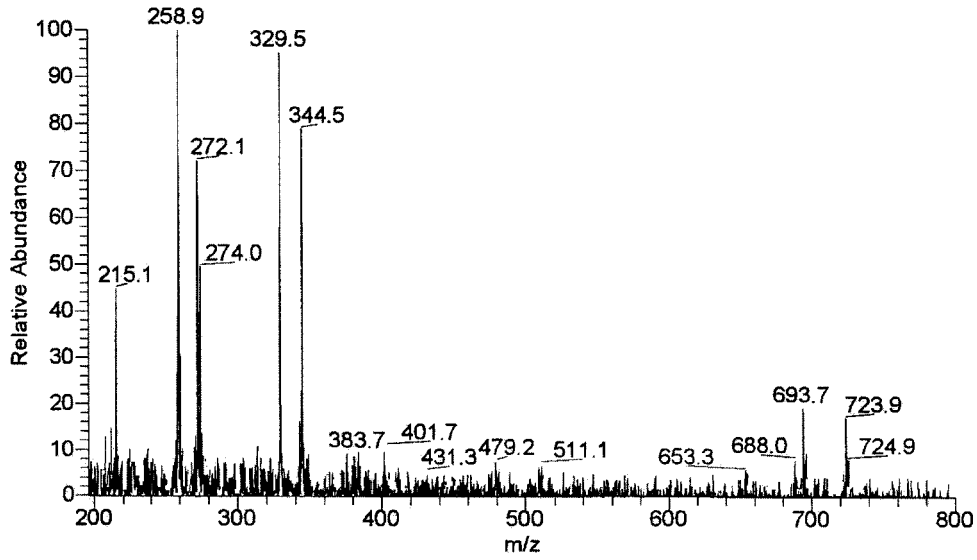

Figure 8. ES-MS of complex **1** in the presence of NaOH and H_2O_2 in methanol; $[MnL^1Cl_2]/NaOH/H_2O_2$ = 1:2:8

Table 7. Peak assignment of complex **1** in the presence of NaOH and H_2O_2 in MeOH; $[MnL^1Cl_2]/NaOH/H_2O_2$ = 1:2:8

m/z (%)	Species
258.9 (100)	$[L^1{}_2Mn^{II}{}_2(\mu\text{-}OH)_2 + H_2O + MeOH + H^+]^{3+}$
329.5 (95)	$[L^1{}_2Mn^{III}{}_2(\mu\text{-}O)_2]^{2+}$
344.5 (78)	$[L^1{}_2Mn^{II}{}_2(\mu\text{-}OH)_2 + 1.5H_2O]^{2+}$
272.1 (72)	$[L^1{}_2Mn^{III}{}_2(\mu\text{-}OH)_2 + 3Cl^- + 2.5H_2O + 2H^+]^{3+}$
215.1 (45)	$[L^1{}_2Mn^{II}{}_2(\mu\text{-}OH)]^{3+}$
693.7 (18)	$[L^1{}_2Mn^{II}{}_2(\mu\text{-}OH)(\mu\text{-}O) + MeOH]^+$
723.9 (17)	$[[L^1{}_2Mn^{II}Mn^{III}(\mu\text{-}O)_2 + 2MeOH]^+$

Table 8. Peak assignments for complex **2** in the presence of NaOH and H_2O_2 in MeOH; $[MnL^2Cl]ClO_4{\cdot}MeOH/NaOH/H_2O_2$ = 1:2:8

m/z (%)	Species
177.1 (100)	$[L^2Mn^{II} + 3H_2O + MeOH + H^+]^{3+}$
418.0 (76)	$[L^2{}_2Mn^{III}{}_2(\mu\text{-}OH) + 2ClO_4^- + 3MeOH + 3H_2O]^{3+}$
287.3 (65)	$[L^2Mn^{IV}(OH)_2 + 3MeOH]^{2+}$
404.3 (32)	$[L^2{}_2Mn^{III}{}_2(\mu\text{-}OH)_2 + 2ClO_4^- + 5H_2O + H^+]^{3+}$
319.1(24)	$[L^2{}_2Mn^{III}Mn^{IV}(\mu\text{-}OH)\ (\mu\text{-}O) + Cl^-]^{3+}$
215.1 (24)	$[L^2Mn^{III} + 2ClO_4^- + 2H^+]^{3+}$
386.1 (19)	$[L^2{}_2Mn^{III}Mn^{IV}(\mu\text{-}O) + 2ClO_4^- + 3H_2O]^{3+}$

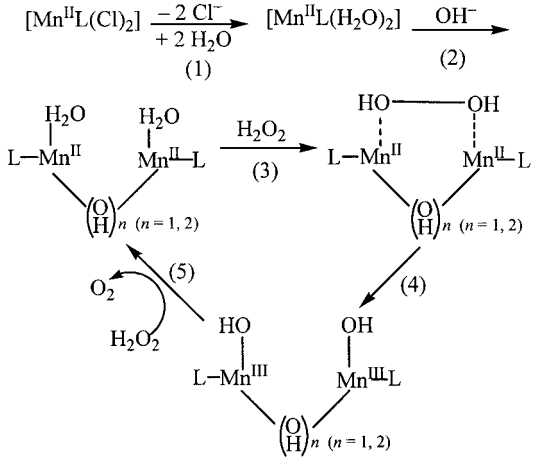

Scheme 1. The mechanism of hydrogen peroxide dismutation by complex **1**

which is close to physiological conditions, complexes **1** and **2** decompose 90% of H_2O_2 during the first 15 min (Figure 7). Therefore, we consider that at physiological pH values the complexes are able to dismutase $^{\cdot}O_2^-$ and are also able to decompose H_2O_2, depending on the concentration of $^{\cdot}O_2^-$. The SOD activities of the complexes are not high, and this is probably due to the fact that some of the species are hydroxylated or bridged. The mechanism for this and its biological relevance need to be studied further.

Conclusion

Two manganese(II) complexes of 1,4,7-tacn with benzimidazole groups, $[MnL^1Cl_2]$ and $[MnL^2Cl]ClO_4{\cdot}MeOH$, were synthesized and characterized. pH titration was used to investigate their stabilities in solution. The introduction of benzimidazole groups on the backbone of tacn increases the stability of the new complexes relative to the parent, unsubstituted complex. The redox potentials of the complexes obtained from cyclic voltammetry show that they are able to dismutase $^{\cdot}O_2^-$. The oxidation state for manganese of the two complexes changes from +2 to +3, and then from +3 to +2, implying that the catalytic mechanism is just a "ping-pong" reaction. ES mass spectrometric and X-ray structure analyses indicated that the binding of Cl^- with Mn^{II} in the complexes is relatively weak, therefore Cl^- can be attacked by $^{\cdot}O_2^-$. The complexes can also be converted into OH- or O-bridged dinuclear manganese(III) or manga-

nese(IV) complexes, which act as active species to decompose H_2O_2 catalytically.

Experimental Section

Materials: L^1 [1-(benzimidazol-2-ylmethyl)-1,4,7-triazacyclononane] and L^2 [1,4-bis(benzimidazol-2-ylmethyl)-1,4,7-triazacyclonone] were prepared by the reported method.[29] Carbonate-free NaOH for pH titration was obtained by Powell's method.[30] $Mn(NO_3)_2{\cdot}6H_2O$ (Analytic Reagent) was recrystallized from doubly distilled water and the stock solutions were standardized by titration with EDTA. In SOD activity experiments, nitroblue tetrazolium nitrate (NBT) (Biochemical Reagent) and L-methionine (Biochemical Reagent) were used and the solutions were prepared using doubly distilled water. The purity of riboflavin was determind by the literature method.[31] The concentration of stock solution of hydrogen peroxide for catalysis activity assay was measured by titration with standardized $KMnO_4$ solution.

Physical Measurements: Elemental analysis was performed using a Perkin−Elmer 240c analytical instrument. IR spectra were measured as KBr discs using a Nicolet 5DX FT-IR spectrophotometer. Electronic spectra were recorded on a UV-3100 spectrophotometer. X-band EPR spectra were measured on an EMX spectrometer in 1.0×10^{-2} mol·dm^{-3} MeOH solution. The electrical conductivity of solutions was measured with a BSD-A conductometer (Jiangsu, P. R. China) with a solution concentration of about 1.0×10^{-3} mol·dm^{-3} in MeCN at 25 ± 0.1 °C. The electrospray mass spectra were determined on a Finnigan LCQ mass spectrograph. The samples (about 0.1 mmol·dm^{-3} in MeOH) were electrosprayed at a flow rate of 5×10^{-6} mol·min^{-1} with a needle voltage of +4.5 kV. The temperature of the heated capillary at the interface was 200 °C and a fused-silica sprayer was used. The mobile phase was an aqueous solution of methanol (1:1, v/v). The samples were run in the positive-ion mode.

Electrochemical Measurements: The cyclic voltammogram experiments were carried out on a PAR Model 273 potentiostat coupled to a PAR Model 175 universal programmer under highly pure nitrogen at 25 ± 0.1 °C. A glassy-carbon electrode was employed as working electrode, a saturated calomel electrode (SCE) as reference electrode, and a platinum wire as auxiliary electrode. The concentration of complex 1 was 1.0×10^{-3} mol·dm^{-3} in 0.1 mol·dm^{-3} $NaClO_4$ aqueous solution and that of complex 2 was 1.0×10^{-3} mol·dm^{-3} in 0.1 mol·dm^{-3} TBAP (tetrabutylammonium perchlorate) MeOH solution. The solutions were deaerated for about 15 min before applying the voltage. The half-wave potentials, $E_{1/2}$, were calculated approximately from $(E_{pa} + E_{pc})/2$ and the measured errors were ±2 mV. Unless otherwise stated, all potentials reported are referenced to the saturated calomel electrode.

pH Titration: Protonation constants of the ligands and stability constants of the complexes were determined by using a Corning pH meter with a glass/silver/silver chloride combination electrode with a precision of ±0.001 pH units. The electrode was standardized against buffer solutions of potassium hydrogen phthalate and sodium borate. The concentrations of ligands ($L^1{\cdot}3HCl$ or $L^2{\cdot}3HCl$) was about 0.0025 mol·dm^{-3}, and the molar ratio of $L^1{\cdot}3HCl$ or $L^2{\cdot}3HCl$ to $Mn(NO_3)_2$ was 1:1. The experimental solutions were titrated with carbonate-free 0.0825 mol·dm^{-3} NaOH by using a microsyringe with a precision of ±2 μL under a nitrogen atmosphere in a sealed jacketed vessel at 25 °C. The ionic strength was kept at 0.1 mol·dm^{-3} by adding KNO_3. For the L^2 systems a dioxane/water mixture (7:3) was used as the solvent and 0.1 mol·dm^{-3} KNO_3 as the support electrolyte as the formed product was not soluble in water.

The equilibria in the systems can be represented by Equation (1)

$$qM + pH + rL \rightleftarrows M_qH_pL_r, \text{ where } \beta_{pqr} = [M_qH_pL_r]/[M]^q[H]^p[L]^r \quad (1)$$

where q, p, and r denote the number of metal ions (M), hydrogen ions (H) and ligand molecules (L) bound in the complex, respectively. A negative p value shows that hydrogen ion is released during coordination. The protonation constants of the ligands were calculated with the PKAS program.[31] Applying the law of mass action to each experimental point i (i = 1, 2, 3...n) gives Equations (2)−(4):

$$C_{Hi} = [H]_i + \sum_{j=1}^{m} p_j \beta_{pjqjrj} [H]_i^{pj} [M]_i^{qj} [L]_i^{rj} \quad (2)$$

$$C_{Mi} = [M]_i + \sum_{j=1}^{m} q_j \beta_{pjqjrj} [H]_i^{pj} [M]_i^{qj} [L]_i^{rj} \quad (3)$$

$$C_{Li} = [L]_i + \sum_{j=1}^{m} r_j \beta_{pjqjrj} [H]_i^{pj} [M]_i^{qj} [L]_i^{rj} \quad (4)$$

where j denotes the ordinal number of complexes (j = 1, 2...m) and C_{Hi}, C_{Mi}, and C_{Li} denote the total concentrations of hydrogen ions, metal ions and ligands in solution, respectively, at each experimental point i.

The equilibrium constants of the complexes were calculated by using the program LEMIT,[32] which is based on the Newton−Raphson and Gauss−Newton method for minimizing U in Equation (5), where C_{Hi}^{calc} and C_{Hi}^{expt} denote the calculated and experimental values of H^+ concentration at the ith point.

$$U = \sum_{i}^{n} (C_{Hi}^{calc} - C_{Hi}^{expt})^2 \quad (5)$$

Crystal-Structure Determination: X-ray intensity data for the manganese(II) complexes were collected on a SMART-CCD area-detector diffractometer. Data reduction and cell refinement were performed with the programs SMART and SAINT.[33] The absorption corrections were carried out by an empirical method. The structures were solved by direct methods (Bruker Shelxtl) and refined on F^2 by full-matrix least-squares (Bruker Shelxtl) using all unique data.[34] The non-H atoms in the structures were subjected to anisotropic refinement. Hydrogen atoms were located geometrically and treated with the riding mode. In $[MnL^2Cl]{\cdot}ClO_4{\cdot}CH_3OH$, the ClO_4^- anion was disordered.

CCDC-233744 (**1**) and -233743 (**2**) contain the supplementary crystallographic data for this paper. These data can be obtained free of charge at www.ccdc.cam.ac.uk/conts/retrieving.html or from the Cambridge Crystallographic Data Centre, 12 Union Road, Cambridge CB2 1EZ, UK [Fax: +44-1223-336-033; E-mail: deposit@ccdc.cam.ac.uk].

Assay of Superoxide Dismutase Activity: The activities were assayed by photoreduction of riboflavin.[24] The solutions contained riboflavin (3.4×10^{-6} mol·dm^{-3}), methionine (0.01 mol·dm^{-3}), nitroblue tetrazolium nitrate (NBT; 4.66×10^{-5} mol·dm^{-3}) and the complexes of various concentrations were prepared with phosphate buffer (pH 7.4). They were illuminated by a fluorescent lamp with a constant light intensity at 25 °C. The optical absorbance (A) of the solutions at 560 nm were measured with various illumination periods (t). Each solution was measured in two parallel tests. Inhibition percentage (I%) was calculated according to the reported

method.[35] The activity (IC_{50}) was defined as the necessary concentration to inhibit 50% reduction of NBT.

Disproportionation of Hydrogen Peroxide:[25,26] An aqueous solution of H_2O_2 (0.5 mL, 3.08 mol·dm^{-3}) was added to a flask containing an aqueous solution of complex **1** or a solution of complex **2** (2.0 mL, 1.22×10^{-3} mol·dm^{-3}) in a methanol/water mixture (1:5). The mixture was stirred and thermostatted at 25 °C, and the O_2 evolved was followed manometrically. To investigate the effect of basicity on the disproportionation of H_2O_2, NaOH solutions of various concentration were added to the flask, the total volumes of solutions were kept to be 2.88 mL for each experiment.

[MnL^{1}Cl$_2$] (1): Manganese(II) acetate (91 mg, 0.34 mmol) was added to a methanol solution (20 mL) of L^1·3HCl·MeOH (125 mg, 0.31 mmol) in 10 mL of methanol. The mixture was stirred for 5 h at room temperature and then filtered. Slow evaporation of the solution gave a pink crystalline compound. Crystals suitable for X-ray diffraction were obtained by diffusion of diethyl ether into an MeCN solution over one week. Yield: 72 mg (61%). $C_{14}H_{21}Cl_2MnN_5$: calcd. C 43.65, H 5.50, N 18.18; found C 43.97, H 5.97, N 18.45. IR (KBr): $\tilde{\nu}$ = 3415 [s, ν(N−H)], 755 cm^{-1} [m, δ(Ph−H)]. UV/Vis (MeOH): λ_{max} = 279 nm (9469 dm^3·mol^{-1}·cm^{-1}), 272 (9150), 268 (8654), 243 (6704). Ω_m (MeCN, 298.2 K): 96.60 S·cm^2·mol^{-1}. μ (290.3 K): 5.63 μ_B.

[MnL^{2}Cl]·ClO$_4$·CH$_3$OH (2): Manganese(II) perchlorate (83 mg, 0.23 mmol) was added to a methanol solution (20 mL) of L^2·3HCl·H$_2$O·1.5EtOH (120 mg, 0.21 mmol) in 10 mL of methanol. Under stirring, the mixture was adjusted to pH 5.0 by addition of a methanol solution of sodium hydroxide. After refluxing for 2 h, the mixture was cooled and filtered. Yellow crystals were isolated from the solution. Yield 69 mg (55%). $C_{23}H_{31}Cl_2MnN_7O_5$: calcd. C 43.13, H 4.93, N 15.17; found C 43.18, H 5.11, N 15.87. IR (KBr): $\tilde{\nu}$ = 3384 cm^{-1} [s, ν(N−H)]; 1108 [s, ν(ClO$_4^-$)], 748 [m, δ(Ph−H)]. UV/Vis (CH_3CN): λ_{max} = 311 nm (416 dm^3·mol^{-1}·cm^{-1}), 279 (12365), 272 (11654), 244 (9846). Ω_m (MeCN, 298.2 K): 100.45 S·cm^2·mol^{-1}. μ (290.3 K): 5.75 μ_B. Crystals suitable for X-ray diffraction analysis were obtained by diffusion of diethyl ether into an MeCN solution over two weeks. Crystallographic data are given in Table 9.

Table 9. Crystal data of complexes **1** and **2**

Complexes	[MnL^{1}Cl$_2$]	[MnL^{2}Cl]ClO$_4$·MeOH
Empirical formula	$C_{14}H_{21}Cl_2MnN_5$	$C_{23}H_{31}Cl_2MnN_7O_5$
Mol. mass	385.20	611.39
Crystal system	monoclinic	monoclinic
Space group	$P2_1/c$	$P2_1/c$
a (Å)	11.208(2)	12.3140(10)
b (Å)	7.6500(10)	14.6130(10)
c (Å)	20.817(3)	15.9340(10)
α (°)	90	90
β (°)	104.900(10)	99.07(2)
γ (°)	90	90
U (Å^3), Z	1724.9(5), 4	2831.4(4), 4
D_c (g·cm^{-3})	1.483	1.434
2θ range (°)	4.0−50	4.4-50
T (K)	293	293
μ(Mo-K_α) (mm^{-1})	1.078	0.701
F(000)	796	1268
Reflections collected	8534	14224
Independent reflections	3020	4978
R indices	0.050	0.021
Observed data [$I > 2\sigma(I)$]	1824	3975
S	0.97	1.03
Final $R1$, $wR2$ [$I > 2\sigma(I)$]	0.0426, 0.0610	0.0527, 0.1481
(all data)	0.0729, 0.0633	0.0641, 0.1535

Acknowledgments

This project was supported by the National Natural Science Foundation of China.

[1] [1a] R. Krämer, *Angew. Chem. Int. Ed.* **2000**, *39*, 4469. [1b] M. McCord, I. Fridovich, *J. Biol. Chem.* **1969**, *244*, 6049.
[2] M. Pick, I. Roboni, J. Fridovich, *J. Am. Chem. Soc.* **1974**, *96*, 7329.
[3] R. Hage, *Recl. Trav. Chem. Pays-Bas.* **1996**, *115*, 385.
[4] V. L. Pecoraro, M. J. Baldwin, A. Gelasco, *Chem. Rev.* **1994**, *94*, 807.
[5] K. Wieghardt, *Angew. Chem. Int. Ed. Engl.* **1989**, *28*, 1153.
[6] W. C. Stallings, K. A. Pattridge, R. A. Strong, M. L. Ludwig, *J. Biol. Chem.* **1985**, 1624.
[7] V. V. Barynin, A. I. Grebenko, *Dokl. Akad. Nauk. SSR.* **1986**, *285*, 1100.
[8] G. C. Dismukes, *Chem. Rev.* **1996**, *96*, 2909.
[9] [9a] C. E. Dube, D. W. Wright, W. H. Armstrong, *Angew. Chem. Int. Ed.* **2000**, *39*, 2169. [9b] A. Gelasco, S. Bensiek, V. L. Pecoraro, *Inorg. Chem.* **1998**, *37*, 3301.
[10] [10a] J. F. Boe, J. J. Girerd, C. Guignard, J. L. Seŕis, J. B. Verlhac, patent no 94/00234, **1994**. [10b]R. Hage, J. E. Iburg, J. Kerschner, J. H. Koek, E. J. M. Lempers, R. J. Martens, U. S. Racherla, S. W. Russell, T. Swarthaff, M. R. P. vanvliet, J. B. Warnaar, L. Van der wolf, B. Krijnen, *Nature* **1994**, *369*, 637.
[11] G. B. Sulpin, G. V. Nizova, Y. N. Kozlov, I. G. Pechenkina, *New J. Chem.* **2002**, *26*, 1238.
[12] D. P. Riley, *Chem. Rev.* **1999**, *99*, 2573.
[13] [13a] D. Salvemini, Z.-Q. Wang, J. L. Zweier, A. Samouilov, H. Macarthur, T. P. Misko, M. G. Currie, S. Cuzzocrea, J. A. Sikorski, D. P. Riley, *Science* **1999**, *286*, 209−210. [13b] D. Riley, K. Udipi, R. Ornberg, *Chem. Brit.* **2000**, 43−44.
[14] [14a] M. Baudry, S. Etienne, A. Bruce, M. Palucki, E. Jacobsen, B. Malfroy, *Biochem. Biophys. Res. Commun.* **1993**, *192*, 964. [14b] Z.-X. Liu, G. B. Robinson, E. M. Gregory, *Arch. Biochem. Biophys.* **1994**, *315*, 74.
[15] [15a] R. F. Pasternack, A. Banth, J. M. Pasternack, C. S. Johnson, *J. Inorg. Biochem.* **1981**, *15*, 261. [15b] L. Batinic-Haberie, L. Benov, I. Spasojevic, I. Fridovich, *J. Biol. Chem.* **1998**, *273*, 2452. [15c] S. Cuzzocrea, B. Zingarelli, G. Castantino, A. P. Caputi, *Free Radic. Biol. Med.* **1999**, *26*, 26.
[16] [16a] D. P. Riley, P. J. Lennon, L. Neumann, R. H. Weiss, *J. Am. Chem. Soc.* **1997**, *119*, 6522. [16b] D. P. Riley, S. L. Henke, P. J. Lennon, K. Aston, *Inorg. Chem.* **1999**, *39*, 1908.
[17] [17a] C. Policar, S. Durot, F. Lambert, M. Cesario, F. Ramiandrasoa, I. Morgenstern-Badarau, *Eur. J. Inorg. Chem.* **2001**, 1807. [17b] D. Salvemini, C. Muscoli, D. P. Riley, S. Cuzzocrea, *Pulm. Thera.* **2002**, *15*, 439.
[18] [18a] R. Bianca, N. Wayman, M. McDonald, A. Pinto, M. Shape, P. Chatterjee, C. Thiemermann, *Med. Sci. Monit.* **2002**, *8*, 1−7. [18b] K. Pong, Y. Rong, S. R. Doctrow, M. Baudry, *Bran Res.* **2002**, *950*, 218. [18c] S. Melov, J. Ravenscroft, S. Malik, M. S. Gill, D. W. Walker, P. E. Clayton, D. C. Wallace, B. Malfroy, S. R. Doctrow, G. J. Lithgow, *Science* **2000**, *289*, 1567.
[19] [19a] S. R. Doctrow, K. Huffman, C. B. Marcus, W. Muslch, A. Bruce, M. Baudry, B. Malfroy, *Adv. Pharmacol.* **1997**, *38*, 247. [19b] K. Baker, C. B. Marcus, K. Huffman, *J. Pharmacol. Exp. Ther.* **1998**, *284*, 215.
[20] C. Jung, Y. Rong, S. Doctrow, M. Baudry, B. Malfroy, Z. Xu, *Neurosci. Lett.* **2001**, *304*, 157.
[21] [21a] S. J. Brudenell, L. Spiccia, A. M. Bond, G. D. Fallon, D. C. R. Hockless, G. Lazarev, P. J. Mahon, E. R. T. Tiekink,

Inorg. Chem. **2000**, *39*, 881. [21b] P. Chaudhuri, K. Wieghardt, *Prog. Inorg. Chem.* **1987**, *35*, 329. [21c] P. V. Bernhardt, G. A. Lawrance, *Coord. Chem. Rev.* **1990**, *104*, 297.
[22] Z. L. Wang, Q. H. Luo, C. Y. Duan, C. Y. Shen, Y. Z. Li, *Dalton Trans.* **2004**, 1104.
[23] D. T. Sawyer, J. S. Valentine, *Acc. Chem. Res.* **1981**, *14*, 393.
[24] C. Beauchamp, I. Fridovich, *Anal, Biochem.* **1971**, *44*, 276.
[25] J.-J. Zhang, Q.-H. Luo, C.-Y. Duan, Z.-L. Wang, Y.-H. Mei, *J. Inorg. Biochem.* **2001**, *86*, 573.
[26] [26a] J.-J. Zhang, Y.-Y. Tang, Q.-H. Luo, C.-Y. Duan, Z.-L. Wang, Y.-H. Mei, *Polyhedron* **2001**, *20*, 2285. [26b] A. E. M. Boelrijk, G. C. Dismukes, *Inorg. Chem.* **2000**, *39*, 3020.
[27] E. J. Larson, V. L. Pecoraro, *J. Am. Chem. Soc.* **1991**, *113*, 3810.
[28] U. Bossek, M. Saher, T. Weyhermuller, K. Wieghardt, *J. Chem. Soc., Chem. Commun.* **1992**, 1780.
[29] Y. Naruta, K. Maruyama, *J. Am. Chem. Soc.* **1991**, *113*, 3595.
[30] Q.-X. Li, Q.-H. Luo, Y.-Z. Li, C.-Y. Duan, Q.-Y. Tu. *Inorg. Chim. Acta*, in press.
[31] J. E. Powell, M. A. Hiller, *J. Chem. Educ.* **1957**, *34*, 330.
[32] A. E. Martell, R. J. Motekaitis, *Determination and Use of Stability Constants*, 2nd ed., VCH Publishers, New York, **1992**, 129.
[33] [33a] Q.-H. Luo, M.-C. Shen, Y. Ding, X.-L. Bao, A.-B. Dai, *Talanta* **1990**, *37*, 357. [33b] J. J. Zhang, Q.-H. Luo, D.-L. Long, J.-T. Chen, F.-M. Li, A.-D. Liu, *J. Chem. Soc., Dalton Trans.* **2000**, 1893.
[34] *SMART and SAINT. Area Detector Control and Integration Software. Siemens Analytical X-ray Systems*, Inc., Madison, Wisconsin, USA, **1996**.
[35] G. M. Sheldrick, *SHELXTL V5.1 Software Reference Manual, Bruker AXS*, Inc., Madison, Wisconsin, USA, **1997**.
[36] Q.-H. Luo, Q. Lu, A.-B. Dai, L.-G. Huang, *J. Inorg. Biochem.* **1993**, *51*, 655.

Received February 25, 2004
Early View Article
Published Online September 23, 2004

